

SPG MITTEILUNGEN COMMUNICATIONS DE LA SSP

AUSZUG - EXTRAIT

Progress in Physics (71)

New magnetic two-dimensional semiconducting layered materials for spintronic applications

Zurab Guguchia and Alex Amato, Laboratory for Muon Spin Spectroscopy, Paul Scherrer Institute

This article has been downloaded from:
https://www.sps.ch/fileadmin/articles-pdf/2020/Mitteilungen_Progress_71.pdf

© see https://www.sps.ch/bottom_menu/impressum/

Progress in Physics (71)

New magnetic two-dimensional semiconducting layered materials for spintronic applications

Zurab Guguchia and Alex Amato, Laboratory for Muon Spin Spectroscopy, Paul Scherrer Institute

Introduction

Spintronics, or spin-based electronics, is one of the promising next generation information technology. It makes use of the quantum property of electrons, such as spin [1, 2], as information carriers and possesses potential advantages like speeding up the data processing, high circuit integration density, and low energy consumption. Magnetic semiconductors, combining the properties and advantages of both magnets and semiconductors, form the basis for spintronics. All semiconductor spintronic devices act according to the following simple scheme: information is stored (written) into spins as a particular spin orientation; the spins, being attached to mobile electrons, carry the information along a wire; and the information is read and processed at a terminal. But spintronics applications require novel magnetic semiconducting materials, which can be produced as very stable thin layers and incorporated in the devices.

Along these lines, transition metal dichalcogenides (TMDs), a family of two dimensional (2D) layered materials like graphene, have appeared as the most promising platforms due to their exciting mechanical, electronic and optoelectronic properties [3 – 9]. TMDs share the same formula, MX_2 , where M is a transition metal and X is a chalcogen. They have a layered structure and crystallize in several polytypes, including $2H$ -, $1T$ -, $1T'$ - and T_d -type lattices. Much interest is focused on the cases where the transition metal M is either Molybdenum (Mo) or Tungsten (W). Hence, the $2H$ forms of these compounds are semiconducting and can be mechanically exfoliated to a monolayer. The unique properties of the TMDs, especially in the monolayer form, have triggered a wealth of device applications such as: magnetoresistance and spintronics, high on/off ratio transistors, optoelectronics, valley-optoelectronics, superconductors and hydrogen storage. Many of these interesting properties arise due to the strong spin-orbit interaction present in these materials arising from the presence of the heavy metal ion. While there are many studies focused on the spin-orbit coupling and the interesting consequences for electrical and optical properties in these materials, there are very limited, and mostly theoretical, studies on the intrinsic magnetism [10 – 12]. Theoretical and experimental work shows that,

in the absence of crystalline imperfections, the Mo-based TMDs are nonmagnetic.

Combining a wealth of different technique, in particular the muon-spin rotation/relaxation technique, we discovered [9] novel magnetism in these very stable semiconducting materials: molybdenum ditelluride ($MoTe_2$) and molybdenum diselenide ($MoSe_2$). In the same materials, we detect the presence of intrinsic dilute self-organized magnetic tellurium/selenium antisite defects (irregularities in the arrangement of atoms) using scanning tunneling microscopy measurements, a finding that is well supported by calculations based on Coulomb corrected density functional theory, a method that models and studies the structure of complex systems with many electrons.

Methods

We studied, both polycrystalline and single-crystalline, samples of $2H$ - $MoTe_2$ and $2H$ - $MoSe_2$ by means of powerful experimental techniques such as muon spin relaxation/rotation (μ SR) [13], scanning tunneling microscopy (STM) and X-ray pair distribution function (PDF) experiments. Hubbard-corrected density functional theory calculations (DFT + U) were also used to gain insights into the experimental results. μ SR

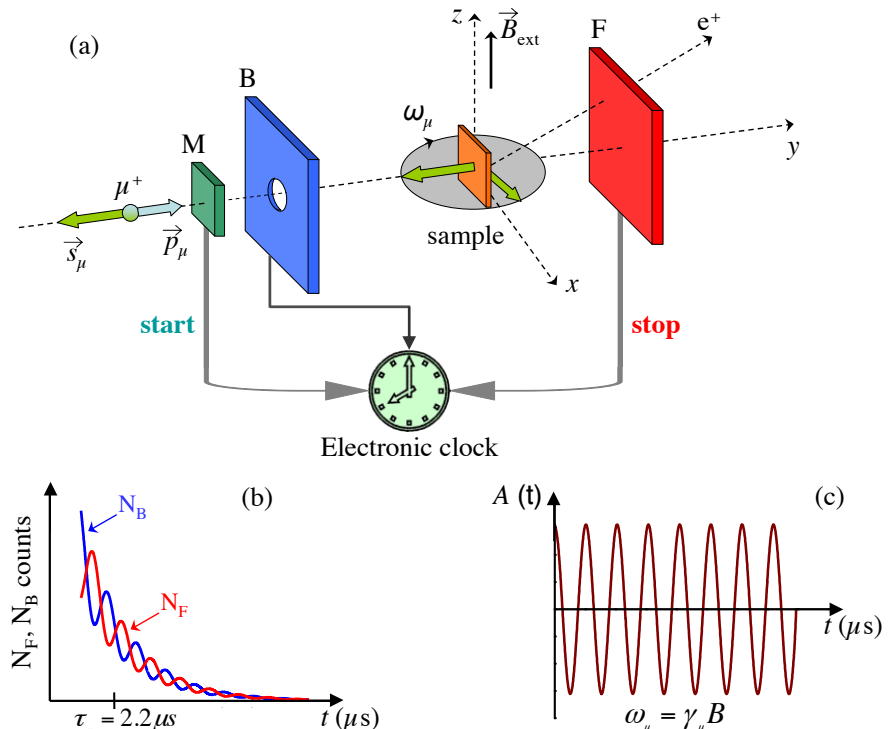


Fig. 1: Principle of a μ SR experiment. (a) Overview of the experimental setup. Spin polarized muons with spin \vec{S}_μ antiparallel to the momentum \vec{p}_μ are implanted in the sample placed between the forward (F) and the backward (B) positron detectors. A clock is started at the time the muon goes through the muon detector (M) and is stopped as soon as the decay positron is detected in the detectors F or B. (b) The number of detected positrons N_F and N_B as a function of time for the forward and backward detector, respectively. (c) The so-called asymmetry (or μ SR) signal is obtained by essentially building the difference between N_F and N_B .

experiments serve as an extremely sensitive local probe technique to detect small internal magnetic fields and ordered magnetic volume fractions in magnetic materials. We also used a unique high-pressure μ SR instrument to study the magnetic properties under hydrostatic pressure [14, 15]. STM has the ability to measure atomic and electronic structure with atomic resolution, and has been used extensively in the past to study local electronic properties in TMDs and other 2D materials [16]. The techniques of STM and μ SR complement each other ideally, as we are able to study the magnetic properties of these crystals sensitively with μ SR experiments and correlate these magnetic properties with atomic and electronic structure measured by STM. The results are published in a journal of the American Association for the Advancement of Science [see Ref. 9].

Muon Spin Rotation Technique

In a μ SR experiment, spin-polarized muons μ^+ are implanted into the sample one at a time [13] (see Fig. 1). Muons thermalize very quickly at interstitial lattice sites, where they act as magnetic microprobes. As the muon undergoes a parity-violating decay, the time evolution of the muon spin polarization $P(t)$ of the muon ensemble can be reconstructed by recording the anisotropic emission of the positrons (mu-

on-decay product) which are preferentially emitted along the direction of the muon spin at a moment of the decay.

In a magnetic material, the muon spin precesses in the local field $\mu_0 H_{\text{int}}$ at the muon site with a Larmor frequency directly related to the internal field. Moreover, the μ SR technique has a unique time window (10^{-4} s to 10^{-11} s) for the study of magnetic fluctuations in materials, which is complementary to other experimental techniques such as neutron scattering, NMR or magnetic susceptibility. High sensitivity (because of the large magnetic moment of the muon) to extremely small static magnetic moments (down to 10^{-3} - 10^{-4} μ B) and the broad time window makes μ SR a powerful tool to investigate magnetism in solid state physics. μ SR is also valuable for studying materials in which magnetic order is random or of short range [17].

Results

Zero-field (ZF) μ SR time spectra for single-crystalline sample of MoTe_2 , recorded for various temperatures in the range between 4 and 300 K, are shown in Fig. 2b. At the highest temperature $T = 300$ K, μ SR reveals that nearly the whole sample is in the paramagnetic state. The paramagnetic state causes only a very weak depolarization of the μ SR

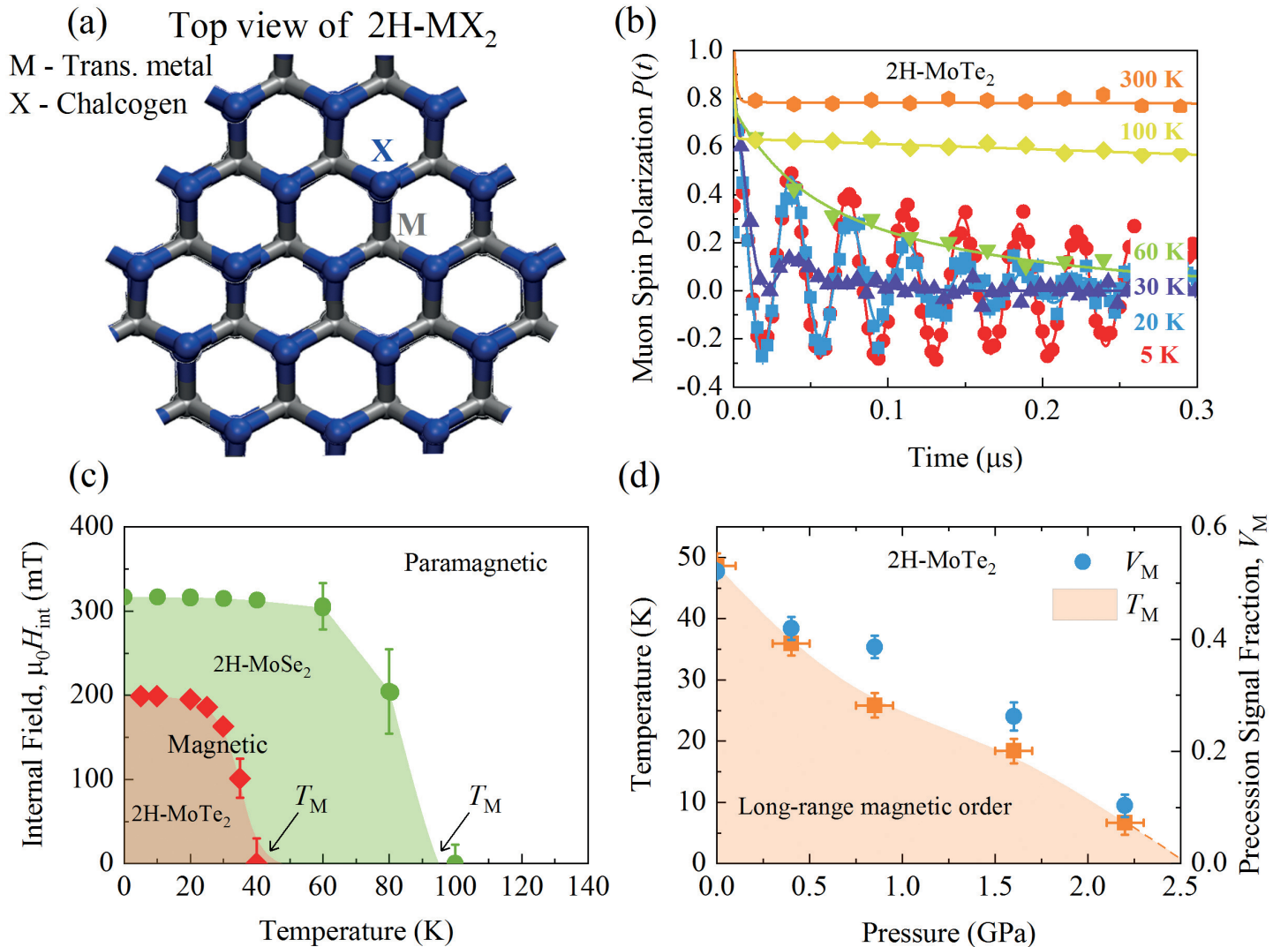


Fig. 2: (a) Hexagonal crystal structure of transition metal dichalcogenide. (b) ZF μ SR time spectra for the single-crystal of 2H-MoTe_2 recorded at various temperatures up to 300 K. (c) Temperature dependence of the internal field $\mu_0 H_{\text{int}}$ of 2H-MoTe_2 and 2H-MoSe_2 as

a function of temperature. (d) Magnetic transition temperature T_M and magnetic volume fraction V_M as a function of pressure [adapted from Ref. 9].

signal. This weak depolarization and its Gaussian functional form originate from the interaction of the muon spin with randomly oriented nuclear magnetic moments. Upon cooling, first, a fast decaying μ SR signal is observed. Below $T_M \simeq 40$ K, in addition to the strongly damped signal, a spontaneous muon spin precession with a well-defined frequency (corresponding to an internal field $\mu_0 H_{\text{int}}$ at the muon site) is observed, which is visible in the raw data (Fig. 2b). Figure 2c shows the temperature dependence of the local magnetic field $\mu_0 H_{\text{int}}$ for MoTe_2 . There is a smooth increase of $\mu_0 H_{\text{int}}$ below $T_M \simeq 40$ K, reaching the saturated value of $\mu_0 H_{\text{int}} = 200$ mT at low temperatures. The observation of a spontaneous muon spin precession is a clear signature of the occurrence of a static and long-range magnetic state in the semiconducting $2H\text{-MoTe}_2$ system below $T_M \simeq 40$ K, and constitutes a remarkable finding. The long-range magnetic order was also observed in the related system $2H\text{-MoSe}_2$ (see Fig. 2c), but with higher ordering temperature $T_M \simeq 100$ K and with higher local magnetic field $\mu_0 H_{\text{int}} \simeq 300$ mT. This difference might be related to the different magnetic structures in $2H\text{-MoSe}_2$ than in $2H\text{-MoTe}_2$. In addition to oscillations, which arises from the precession of the spin of the diamagnetic muon around the internal magnetic field, we observe another component, which exhibits a strong relaxation. In addition, it is evident from the ZF μ SR data that upon cooling, the oscillating component develops at the cost of the strongly damped fraction and both fractions together cover the whole volume of the sample. The strongly damped signal observed in these compounds is

attributed to the presence of a muonium fraction. Muonium, a bound state formed by a positive muon and an electron, may form in semiconductors [17]. In the bound state, the muon is much more sensitive to magnetic fields than as a free probe, because its magnetic moment couples to the much larger electron magnetic moment, thus amplifying the oscillations and the depolarization effects. Therefore, even small variations of the internal magnetic field may cause a strong depolarization such as that observed in the spectra at early times. In any case, the presence of the oscillating signal in the ZF μ SR time spectra in these compounds is a clear signature of magnetism in the nearly full volume of the sample. Moreover, we determined that hydrostatic pressure has a significant effect on the magnetic properties of these materials. Namely, we see both a suppression of the magnetically ordered fraction and a decrease of the magnetic order temperature T_M as a function of pressure (Fig. 2d). This strong pressure dependence of magnetism is very encouraging, because it indicates that one can have control over the magnetic properties. This also means that uniaxial strain, which is another interesting and widely applied tuning parameter, might also be useful in these materials.

Previous theoretical work [11] and simple chemical bonding considerations indicate that the Mo atoms in $2H\text{-MoTe}_2$ are in a nonmagnetic $4d^2$ configuration. We therefore investigated the presence of defects using the high-resolution STM in the crystals measured by μ SR. This STM study indicates the presence of intrinsic dilute defects (see Fig. 3a). Note

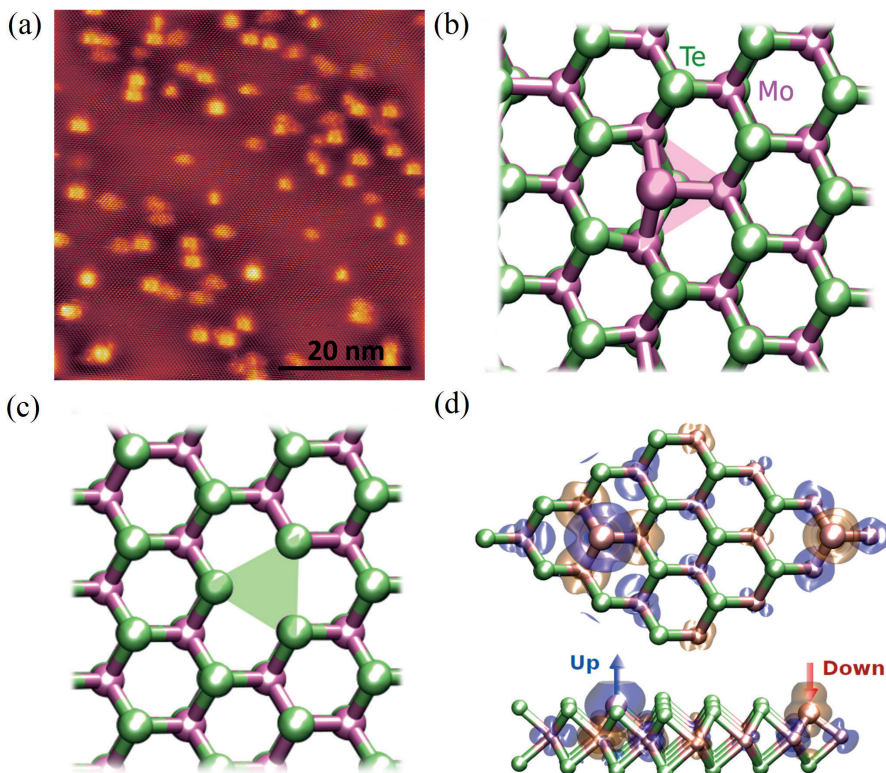


Fig. 3: (a) Large-scale atomic-resolution STM topography (note the 20 nm scale) of the $2H\text{-MoTe}_2$ surface. The image reveals an approximately uniform density of two types of defects over the entire surface. (b) DFT+U-optimized geometry for the chalcogen-antisite Mo_{sub} defect. (c) DFT+U-optimized geometry of the metal-vacancy defect Mo_{vac} . (d) Magnetization density on the top surface of bulk $2H\text{-MoTe}_2$ in the antiferromagnetic configuration. Spin-up and spin-down states are shown in faint blue and orange iso-surfaces, respectively. Note that spins also couple antiferromagnetically at the local level between the chalcogen-antisite defect and the nearest Mo atoms [adapted from Ref. 9].

that two major defects, i.e. chalcogen-antisites (Fig. 3b) (where a molybdenum atom substitutes the Tellurium/Selenium atom) and metal-vacancies (Fig. 3c), were found in these materials synthesized by two different methods - chemical vapor transport and self-flux growth [9]. Commercial samples were also tested and the same types of defects were detected, indicating that defects are truly intrinsic for MoTe_2 and MoSe_2 and that they are randomly distributed in the crystal lattice. Scanning tunneling spectroscopy spectra, taken on the chalcogen-antisites defects (Mo_{sub}) always display a deep in-gap state, while the metal vacancy (Mo_{vac}) does not show such a feature [9].

Having identified the primary defect types in our crystals, we performed Hubbard corrected DFT+U calculations to examine their magnetic properties [18]. DFT indicates that the chalcogen-antisite defects Mo_{sub} are magnetic, while metal-vacancy defects Mo_{vac} do not introduce a significant local moment [9]. The spin-polarized density of states shows that the localized Mo-4d states at the Fermi level carry most of the magnetization with minor contribution from p states of the Te atoms. DFT also determines that the chalcogen-antisite Mo_{sub} defects are coupled antiferromagnetically to the nearest-neighbor Mo atoms, as shown in Fig. 3d. The magnetic moments at the nearest-neighbor Mo atoms can reach 0.10

to $0.40 \mu_B/\text{atom}$, with smaller contributions for second and third neighbors (0.02 to $0.08 \mu_B/\text{atom}$). The Tellurium atoms show negligible spin polarization. Similar effects have previously been observed [18] in graphene with different adsorbates and substitutional metal atoms.

Discussion

Our muon measurements unambiguously establish $2H\text{-MoTe}_2$ and $2H\text{-MoSe}_2$ as intrinsic magnetic, moderate bandgap semiconductors [9]. The μSR results indicate magnetic order below $T_M \simeq 40$ and 100 K for MoTe_2 and MoSe_2 , respectively. In the same materials, STM measurements demonstrate the presence of intrinsic dilute self-organized magnetic Tellurium/Selenium-antisite defects, a finding that is supported by Coulomb corrected DFT. The defects have a large electronic impact. Although the exact link between μSR and STM/DFT results is not yet clear, both results together constitute a first strong evidence concerning the relevance of magnetism in the TMDs physics. At present, one does not understand all the mechanisms at play for the origin of magnetism in these materials. Low-density of the chalcogen-antisite defects cannot give rise to long-range magnetic order, unless these defects have electronic coupling to the semiconductor valence electrons. The presence of such spin-polarized itinerant electrons would imply that these materials are dilute magnetic semiconductors. Recently, ferromagnetism in VSe_2 monolayers was reported, but this system is characterized by a high density of states at the Fermi level [19]. The novelty of our work in $2H\text{-MoTe}_2$ and $2H\text{-MoSe}_2$ is that one observes intrinsic long-range magnetic order and at the same time good semiconducting behavior. To fully exploit the magnetic properties of these TMD semiconductors, future work needs to address these important issues.

Importance of the presence of magnetism in semiconducting TMDs

Previously, dilute magnetic semiconductors have been synthesized in a range of thin film and crystal materials [20, 21]. Much interest has been focused on the III-V semiconductor class, where a small concentration of some magnetic ions, particularly Mn^{2+} , can be incorporated by substituting for the group III cations of the host semiconductor. Numerous technical challenges in making uniform DMS materials have been overcome in recent years, but formidable challenges still remain in producing stable, high-quality DMS materials with high T_c . Our present systems offer an alternative route to synthesize DMS materials with the following advantages:

1. The defects contributing to magnetism are intrinsic in the crystal and are uniformly distributed. This can alleviate some of the materials challenges commonly faced in DMS synthesis.
2. The materials are cleavable down to a monolayer thickness and readily grown in large-area form. As it is well

established in these materials, the bandgap is strongly dependent on the thickness, providing tunability over the semiconductor properties.

3. The chemical potential and electric field in thin films are easily tuned by electrostatic gates, opening the possibility to tune magnetism, as demonstrated in GaAs.
4. Finally, these materials can be easily layered by van der Waals hetero-epitaxy, allowing the creation of unique new device concepts.

Acknowledgements

ZG: When I discovered magnetism in semiconducting $2H\text{-MoTe}_2$ with μSR , I was a postdoc in the Laboratory for Muon Spin Spectroscopy at the Paul Scherrer Institute, Switzerland, working with Dr. Alex Amato and Prof. Elvezio Morenzoni. One month later, with an advanced mobility grant of the SNSF, I joined the group of Prof. Yasutomo Uemura at the Columbia University, where I have carried out systematic studies on these systems in strong collaboration with the group of Prof. Abhay Pasupathy at the Columbia University, Prof. Simon Billinge at the Columbia University and the group of Dr. Elton Santos at the Queens University of Belfast.

AA & ZG: Samples for the initial μSR measurements were provided by Dr. Fabian von Rohr from the University of Zurich. Dr. Daniel Rhodes from the Columbia University provided samples for STM and follow-up μSR experiments. This work benefited from a combination of various experimental techniques and from DFT calculations. The μSR experiments were carried out at the Swiss Muon Source ($S\mu\text{S}$) of the Paul Scherrer Institute. STM and SQUID experiments were carried out at the Columbia University. DFT calculations were performed at the Queens University of Belfast. X-ray PDF experiments were carried out at the Brookhaven National Laboratory. The authors thank all the people involved in this project.

- [1] F. Pulizzi, *Nat. Materials* **11**, 367 (2012).
- [2] O. D. Jayakumar, A. K. Tyagi, Chapter from the book "Functional Materials" <https://doi.org/10.1016/C2010-0-65659-8> (2012).
- [3] A. A. Soluyanov *et al.*, *Nature* **527**, 495–498 (2015).
- [4] X. Xu *et al.*, *Nat. Phys.* **10**, 343–350 (2014).
- [5] M. N. Ali *et al.*, *Nature* **514**, 205–208 (2014).
- [6] X. Qian *et al.*, *Science* **346**, 1344–1347 (2014).
- [7] D. Costanzo *et al.*, *Nature Nanotechnology* **11**, 339 (2016)
- [8] Z. Guguchia *et al.*, *Nat. Commun.* **8**, 1082 (2017).
- [9] Z. Guguchia *et al.*, *Sci. Adv.* **4**: eaat3672 (2018).
- [10] S. Tongay *et al.*, *Appl. Phys. Lett.* **101**, 123105 (2012).
- [11] C. Ataca *et al.*, *J. Phys. Chem. C* **115**, 3934–3941 (2011).
- [12] Y. Li *et al.*, *J. Am. Chem. Soc.* **130**, 16739–16744 (2008).
- [13] A. Amato *et al.*, *Rev. Sci. Instrum.* **88**, 093301 (2017).
- [14] R. Khasanov, Z. Guguchia *et al.*, *High Press. Res.* **36**, 140–166 (2016).
- [15] Z. Guguchia *et al.*, *Nat. Commun.* **6**, 8863 (2015).
- [16] A. Kerelsky *et al.*, *Nano Lett.* **17**, 5962–5968 (2017).
- [17] Z. Salman *et al.*, *Phys. Rev. Lett.* **113**, 156801 (2014).
- [18] E. J. G. Santos *et al.*, *New J. Phys.* **12**, 053012 (2010)
- [19] M. Bonilla *et al.*, *Nature Nanotechnology* **13**, 289 (2018).
- [20] C. Ding *et al.*, *Phys. Rev. B* **88**, 041102(R) (2013).
- [21] T. Dietl *et al.*, *Nat. Mater.* **9**, 965–974 (2010).